Synthesis gas formation by direct oxidation of methane over Rh monoliths ☆

D.A. Hickman [1], E.A. Haupfear and L.D. Schmidt [2]

Department of Chemical Engineering and Materials Science, University of Minnesota, Minneapolis, MN 55455, USA

Received 9 September 1992; accepted 30 November 1992

The production of H_2 and CO by catalytic partial oxidation of CH_4 in air or O_2 at atmospheric pressure has been examined over Rh-coated monoliths at residence times between 10^{-4} and 10^{-2} s and compared to previously reported results for Pt-coated monoliths. Using O_2, selectivities for H_2 (S_{H_2}) as high as 90% and CO selectivities (S_{CO}) of 96% can be obtained with Rh catalysts. With room temperature feeds using air, Rh catalysts give S_{H_2} of about 70% compared to only about 40% for Pt catalysts. The optimal selectivities for either Pt or Rh can be improved by increasing the adiabatic reaction temperature by preheating the reactant gases or using O_2 instead of air. The superiority of Rh over Pt for H_2 generation can be explained by a methane pyrolysis surface reaction mechanism of oxidation at high temperatures on these noble metals. Because of the higher activation energy for OH formation on Rh (20 kcal/mol) than on Pt (2.5 kcal/mol), H adatoms are more likely to combine and desorb as H_2 than on Pt, on which the $O+H \rightarrow$ OH reaction is much faster.

Keywords: Methane oxidation; rhodium catalyzed oxidation of methane; synthesis gas ($CO+H_2$) from methane

1. Introduction

The conversion of methane to more useful and easily transported chemicals is essential if the world's abundant resources of natural gas are to be effectively utilized. In general, methane is converted to synthesis gas via steam reforming,

$$CH_4 + H_2O \rightarrow CO + 3H_2, \quad \Delta H = +49.2 \text{ kcal/mol}. \tag{1}$$

The synthesis gas product is a feedstock for many chemical processes, including the production of methanol and Fischer–Tropsch synthesis. For these two

☆ This research was partially supported by DOE under Grant No. DE-FG02-88ER13878-AO2.

[1] Present address: The Dow Chemical Company, Midland, MI 48674, USA.

[2] To whom correspondence should be addressed.

processes, the desired H_2/CO ratio is ≈ 2, which is exactly the stoichiometry of the direct oxidation reaction

$$CH_4 + \tfrac{1}{2}O_2 \rightarrow CO + 2H_2, \quad \Delta H = -8.5 \text{ kcal/mol}. \tag{2}$$

Because the reforming reaction gives a H_2/CO ratio of 3, additional downstream reactors are required to adjust this ratio by the water–gas shift reaction,

$$CO + H_2O \rightleftharpoons CO_2 + H_2, \quad \Delta H = -9.8 \text{ kcal/mol}. \tag{3}$$

In addition to its more desirable stoichiometry, the direct oxidation reaction is slightly exothermic. The endothermicity of the steam reforming reaction requires energy input, while a reactor based on the exothermic direct oxidation reaction would be more energy efficient.

Another advantage of a direct oxidation process would be that smaller reactors (or higher throughput) would be possible because the direct oxidation reaction is significantly faster than the reforming reaction. Steam reforming reactors typically have superficial contact times (based on the feed gases at STP) on the order of 1 s [1], while a direct oxidation process could have superficial contact times of 10^{-2} s or less [2].

Although thermodynamic equilibrium calculations show that a 2/1 CH_4/O_2 feed is completely converted to a 2/1 H_2/CO mixture at temperatures above ≈ 1000°C, the approach to this equilibrium is slowed by formation of the total oxidation products H_2O and CO_2, leaving *excess* CH_4 in the products. There are several catalytic systems in the literature [3–6] whose equilibrium yields of synthesis gas are attributed to a reaction sequence in which a fraction of the feed CH_4 is converted to H_2O, CO, and CO_2, and the remainder of the CH_4 is converted via reforming reactions.

In this paper, we present results from experiments on autothermal direct oxidation to synthesis gas of fuel-rich CH_4–air or CH_4–O_2 mixtures over Rh-coated Al_2O_3 foam monoliths and compare these results with previously reported data for Pt-coated monoliths [2]. We will contrast the performance of these two catalysts at conditions approaching adiabatic reactor operation and suggest an explanation for the difference based on our understanding of elementary surface reactions on these noble metal surfaces.

Besides comparing the performance of Pt- and Rh-coated catalysts, we will describe the microstructure of these catalysts as observed using scanning electron microscopy (SEM). We will correlate this microstructural information with variations in catalyst selectivity due to the catalyst loading and the catalyst age. Finally, the effect of reactor pressure on product selectivity, especially the formation of C_2 hydrocarbons, will be addressed.

2. Apparatus and procedure

The apparatus and experimental procedure used for these experiments have been described in detail previously [2]. The reactor consists of an 18 mm i.d.

quartz tube into which the cylindrical catalytic monoliths are placed. The reactor is insulated with high temperature silica–alumina insulation outside the tube and radiation shields (noncatalytic monoliths) before and after the catalyst inside the tube. The reactor is operated at a steady-state autothermal temperature which is 50–100°C less than the adiabatic reaction temperature due to heat losses which are unavoidable in a reactor of this size. The product gas composition is monitored by a gas chromatograph and the autothermal temperatures are measured using a chromel–alumel thermocouple located immediately after the catalytic monolith and before the downstream radiation shield.

For these experiments, the noble metals were applied directly to foam monoliths. These monoliths, which are α-Al_2O_3 with an open cellular, sponge-like structure, had nominally 30–50 pores per inch (ppi) and were cut into 17 mm diameter cylinders 2–20 mm long. The catalyst loadings on the monoliths varied from 0.1 to 20 wt% noble metal. The samples with high (> 1%) weight loadings of metal were prepared by a technique involving an organometallic deposition. Scanning electron microscopy (SEM) micrographs of these monoliths before and after use revealed that the catalyst formed large crystallites on the support with the metal covering a significant fraction of the support surface. The samples with lower loadings were prepared by soaking the monoliths in an aqueous salt solution ($Rh(NO_3)_3$ or H_2PtCl_6), drying in air, and then calcining for 4 h at 600°C.

3. Results

3.1. Rh VERSUS Pt

In fig. 1, we compare the H_2 and CO selectivities, fractional CH_4 conversion, and autothermal temperature for two monoliths: a 11.6 wt% Pt, 50 pores per inch (ppi) Al_2O_3 foam monolith 7 mm long, and a 9.8 wt% Rh, 80 ppi Al_2O_3 foam monolith 10 mm long. For each sample, the feed composition was varied while maintaining a fixed total flow rate of 4 standard liters per minute (slpm) and a constant feed gas temperature. Data for feed gas temperatures of 25 and 460°C are shown.

The primary observation is that Rh is a significantly better catalyst for producing H_2 and CO by direct oxidation of methane. With a room temperature feed, the optimal selectivities are $S_{H_2} = 0.43$ and $S_{CO} = 0.89$ for the Pt catalyst compared to $S_{H_2} = 0.73$ and $S_{CO} = 0.90$ for the Rh catalyst, where the selectivities are defined as

$$S_{H_2} = \frac{0.5\,F_{H_2}}{F_{CH_4,in} - F_{CH_4,out}} = \frac{F_{H_2}}{F_{H_2} + F_{H_2O} + 2F_{C_2H_4} + 3F_{C_2H_6}} \tag{4}$$

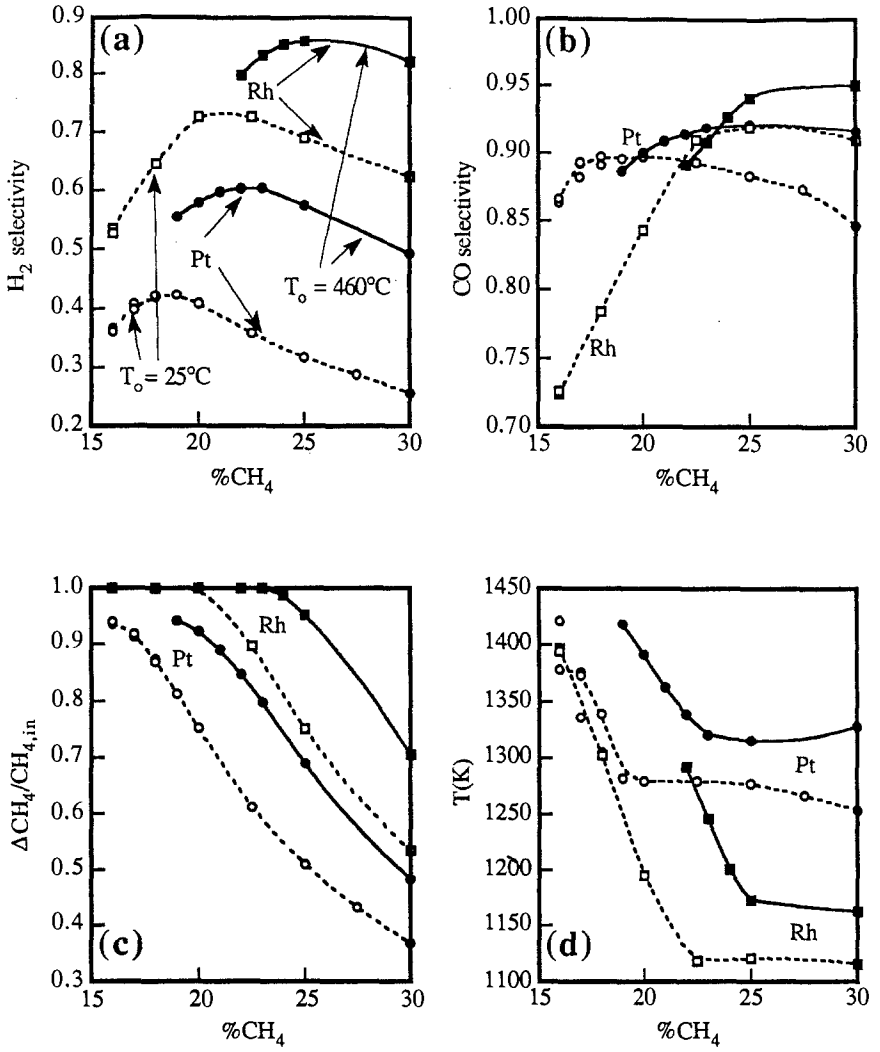

Fig. 1. (a) H_2 and (b) CO selectivities, (c) CH_4 conversions, and (d) autothermal temperatures for a 50 ppi×7 mm, 11.6 wt% Pt monolith and a 80 ppi×10 mm, 9.8 wt% Rh monolith as a function of feed composition and preheat temperature at a total mass flow rate of 4 slpm CH_4 and air. Squares represent Rh, circles represent Pt, open symbols represent a feed temperature of 25°C, and filled symbols represent a feed temperature of 460°C.

and

$$S_{CO} = \frac{F_{CO}}{F_{CH_4,in} - F_{CH_4,out}} = \frac{F_{CO}}{F_{CO} + F_{CO_2} + 2F_{C_2H_4} + 2F_{C_2H_6}}, \quad (5)$$

where F_i is the molar flow rate of species i.

Furthermore, because the Rh catalyst gives better selectivities, the feed composition corresponding to optimal synthesis gas production ($\approx$ 19% CH_4 for

Table 1
Comparisons of monoliths

ID	Monolith	Metal	Loading (wt%)	Cell density [a]	Length (mm)	Feed	CH_4/O_2	S_{H_2}	S_{CO}	$\Delta CH_4/CH_{4,in}$
1	foam	Rh	9.8	80 ppi	10	O_2	1.6	0.86	0.95	0.98
2	foam	Pt	11.6	50 ppi	7	O_2	1.7	0.64	0.89	0.77
3	foam	Rh/Pt	9.9/9.9	40 ppi	7	O_2	1.8	0.72	0.93	0.75
4	foam	Rh	0.56	50 ppi	7	O_2	1.7	0.74	0.93	0.80
5	extruded	Pt	12.0	400 csi	7	air	1.05	0.45	0.82	0.82
6	extruded	Pt	≈ 0.1	400 csi	7	air	1.05	0.13	0.83	0.67

[a] ppi = pores per inch; csi = cells per square inch.

Pt and ≈ 22% for Rh) is closer to the ideal feed composition of 29.6% CH_4 in air.

In addition, both catalysts give higher CH_4 conversions for a given feed composition when the feed gas is preheated since preheating increases the autothermal temperature of the reactor, resulting in higher selectivities of direct formation of H_2 and CO. For both Pt and Rh, the autothermal reactor temperature levels off for compositions with a CH_4/O_2 feed ratio higher than the optimal ratio for H_2 production. Furthermore, because Rh is a more selective catalyst for the only slightly exothermic direct partial oxidation reaction (2), the autothermal reactor temperature is significantly lower (by as much as 250 K) for Rh than for Pt.

In table 1, optimal selectivities are shown for several samples of various catalyst compositions. In addition to the two samples discussed above, a third sample containing 9.9 wt% each Pt and Rh was tested. A comparison of the performance of these three samples confirms that Rh is a better catalyst than Pt for synthesis gas production, especially for H_2 production. Sample 3, with 1/1 Pt/Rh, gives H_2 selectivities significantly higher than sample 2, which has a high loading of Pt, and significantly lower than sample 1, which has a high loading of Rh.

3.2. CATALYST MICROSTRUCTURE AND LOADING

Table 1 also compares optimal selectivities for the samples with 9.8 and 0.56 wt% Rh (samples 1 and 4, respectively), with higher loadings of Rh giving higher H_2 selectivities. Similar results are seen for the Pt-coated extruded monoliths (samples 5 and 6). Comparisons of the microstructure (by SEM) and elemental surface composition (by energy dispersive spectroscopy, EDS) of fresh catalysts with different loadings showed that higher loadings of Pt or Rh resulted in higher ratios of metal to Al on the catalyst surface, and the Al_2O_3 was almost completely covered with ≈ 10 wt% Pt or Rh.

An interesting correlation between catalyst microstructure and activity was

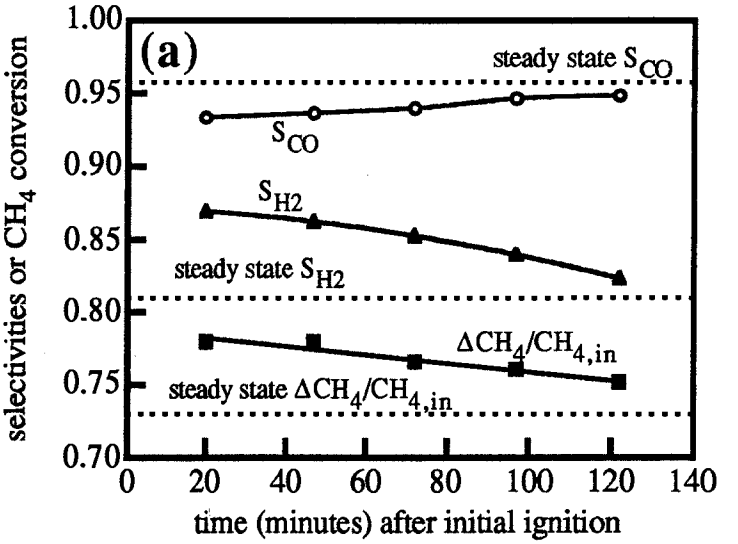

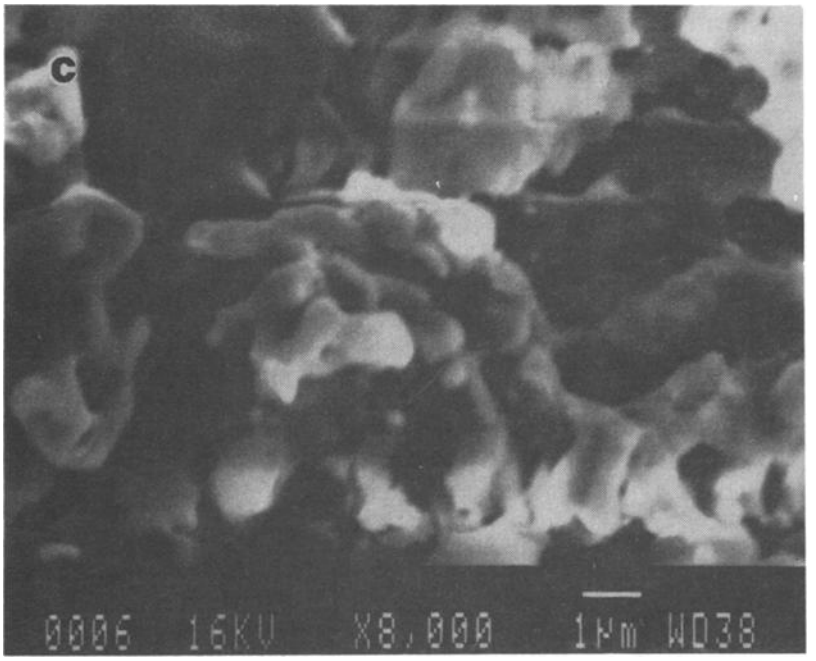

Fig. 2. (a) Selectivities and CH_4 conversion as a function of time after initial ignition of the 9.8 wt% Rh catalyst in fig. 1. Steady-state values are shown by the dashed lines. Micrographs are of the 9.8 wt% Rh-coated foam monolith after several hours of reaction. (b) A typical area on the monolith at a magnification ratio of 1000. (c) is a higher magnification (×8000) view of an area of the catalyst whose elemental composition was primarily Rh. (d) An area whose elemental composition was primarily Al (magnified × 1000).

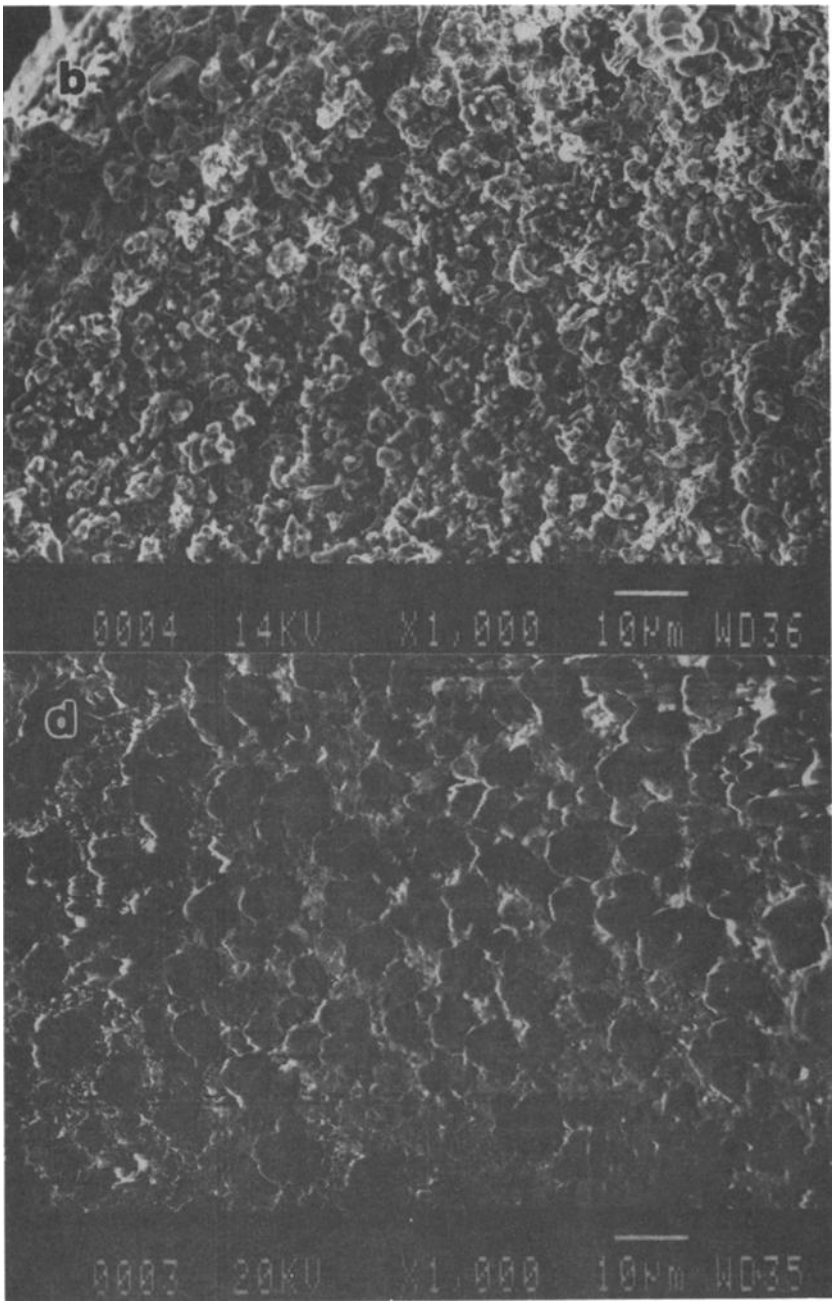

observed for the 9.8 wt% Rh sample. Following the initial ignition of the original, unused catalyst, the product selectivities were monitored for 2 h. As shown in fig. 2, the initial S_{H_2} and $\Delta CH_4/CH_{4,in}$ were slightly higher than the

steady state values observed after several hours of operation, while S_{CO} was initially lower than the eventual steady state value.

Analysis of several different locations on a fresh Rh catalyst with 11.1 wt% Rh by EDS and SEM revealed a fairly uniform coverage of Rh crystallites ≈ 1 μm in diameter which almost completely covered the Al_2O_3 support. However, after several hours of reaction, the catalyst microstructure and surface composition changed significantly. The three micrographs in fig. 2 show the 9.8 wt% Rh sample after several hours of operation at the steady state conversion and selectivities in fig. 2a. Fig. 2b shows a typical area whose elemental composition was determined by EDS to include both Al and Rh. Examination of several different areas on the front face of the monolith revealed that the Rh tended to accumulate in certain areas of the monolith, fig. 2c, while very little Rh was detected in other areas, fig. 2d. As shown in fig. 2c, the Rh appears to sinter into large connected particles with rounded features. Similar microstructural changes were also observed for Pt catalysts.

In general, EDS showed that the ratio of exposed Al to exposed Rh *on the front face of the monolith* increased during the reaction. This must be a consequence of the sintering of the Rh particles and perhaps the migration of the Rh particles to areas located further downstream in a given channel.

After the initial change in catalyst activity described above, all of the monolith catalysts maintained their steady state activities for several hours of use, with no apparent long term deactivation observed. In addition, the initial catalyst deactivation appeared to be irreversible since operating under more oxidizing conditions did not restore the catalyst to its initial activity.

3.3. AIR VERSUS O_2

Data for experiments over the 9.8% Rh sample using both air and O_2 are shown in fig. 3. For all of these experiments, a total flow rate of 4 slpm was maintained with room temperature feed gases. To facilitate comparison of the air and the O_2 experiments, the selectivities and CH_4 conversion are plotted as a function of the CH_4/O_2 ratio. This data reveals that elimination of the N_2 diluent is essentially equivalent to preheating the feed gases to about 460°C for this sample. Preheating the CH_4–O_2 feed further improves the selectivity of H_2 and CO formation to as high as 0.90 and 0.96 respectively.

3.4. HYDROCARBON FORMATION

In fig. 4a, the selectivities of hydrocarbon formation for samples 1–4 are compared as a function of feed composition for a feed containing methane and oxygen. In these and all other experiments, the only products observed besides H_2, H_2O, CO, and CO_2 were C_2H_4 and C_2H_6. The formation of C_2 hydrocarbon byproducts is obviously a function of the catalyst used. The gas chromato-

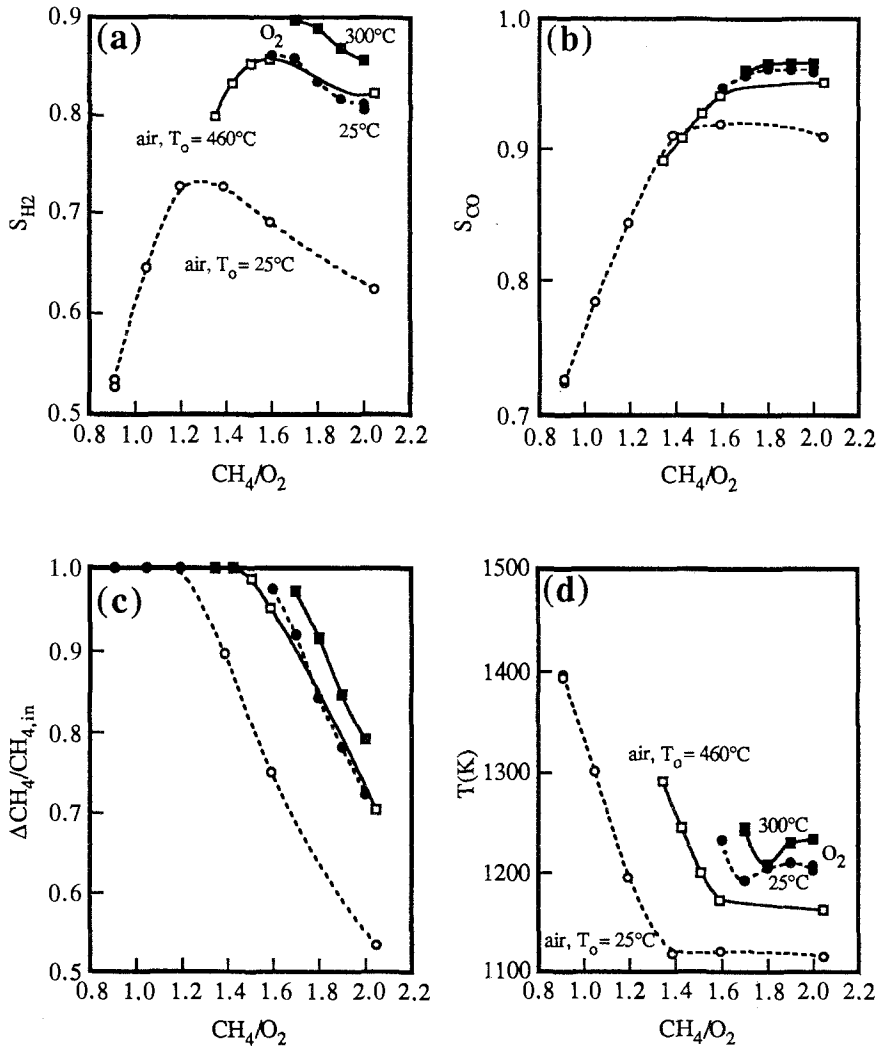

Fig. 3. (a–b) Selectivities, (c) CH_4 conversion, and (d) autothermal temperatures for the 9.8 wt% Rh catalyst using air or O_2 and various feed temperatures at a total flow rate of 4 slpm.

graphic analysis employed in these experiments has a lower detection limit of about 0.02 mol% (corresponding to a hydrocarbon selectivity of $\approx 0.1\%$) for the hydrocarbon species.

A comparison of the production of hydrocarbons with the optimal H_2 and CO selectivities listed for the same samples in table 1 reveals that a catalyst giving better S_{H_2} and S_{CO} gives correspondingly lower hydrocarbon selectivities. In addition, since all of these experiments were conducted at the same total flow rate (4 slpm) and feed temperature (25°C), better S_{H_2} and S_{CO} correspond to lower autothermal reactor temperatures. Thus, the formation of hydrocarbons may be affected by the autothermal reactor temperature or the catalyst.

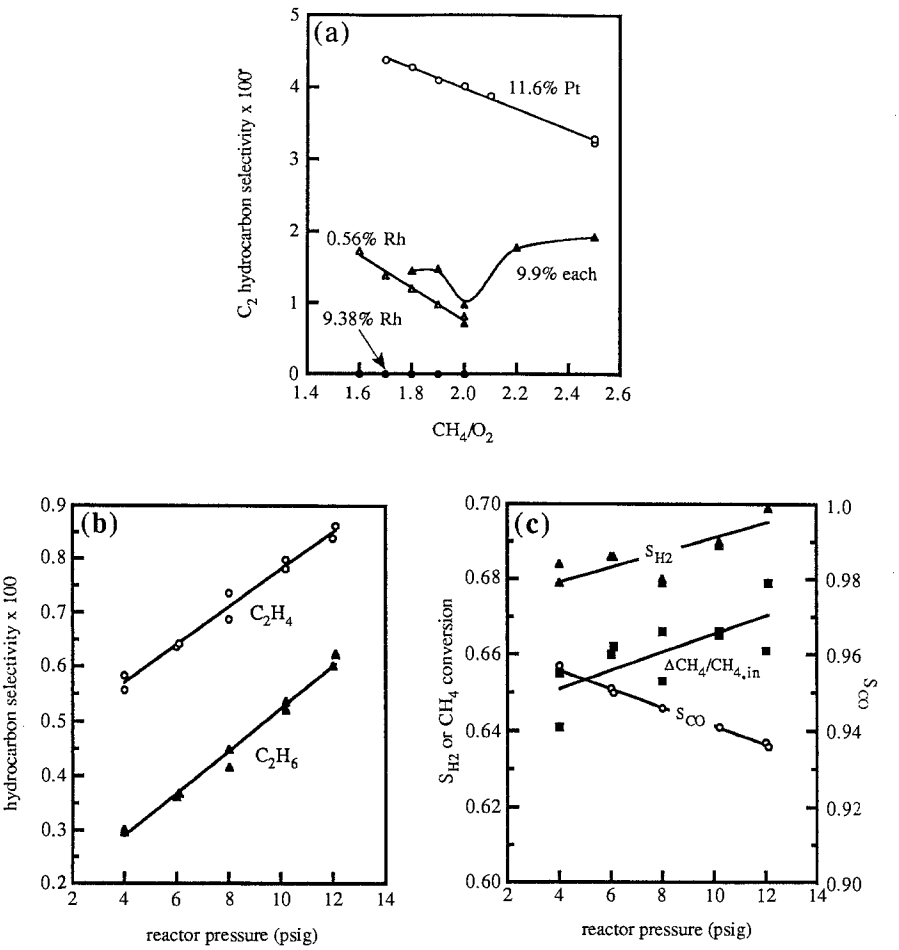

Fig. 4. (a) Overall C_2 hydrocarbon ($C_2H_4 + C_2H_6$) selectivity ($\times 100$) based on carbon atoms as a function of the CH_4/O_2 feed ratio with a total flow rate of 4 slpm over a 40 ppi foam monolith with 9.9 wt% each of Pt and Rh. (b) C_2 hydrocarbon selectivities, (c) S_{H_2}, S_{CO}, and CH_4 conversion as a function of reactor pressure for a fixed mass flow rate of 4 slpm over the same monolith as in (a).

Figs. 4b, 4c demonstrate the effect of reactor pressure on CH_4 conversion, hydrocarbon formation, S_{H_2}, and S_{CO}. Since an industrial synthesis gas process would be likely to operate at pressures as high as 30 atm, it is important to understand the influence of the reactor pressure on product selectivities. Specifically, bimolecular gas phase reactions should have rates proportional to the square of the total pressure, while flux-limited surface reaction rates will increase proportional to the pressure. Thus, if gas phase reactions are significant, their impact will increase with higher reactor pressures.

For these experiments, sample 3 from table 1 was tested for a fixed mass flow rate of 4 slpm and a 2/1 CH_4/O_2 feed at room temperature. As shown in the

figure, increasing the reactor pressure over a range of 4 to 12 psig does have a slight effect on the product selectivities. However, over the entire range of pressures used here, the hydrocarbon selectivity, defined as

$$S_{C_2} = S_{C_2H_4} + S_{C_2H_6}, \tag{6}$$

is more than two orders of magnitude smaller than S_{H_2} and S_{CO}. As the pressure increases, S_{H_2}, and S_{C_2} increase slightly, while S_{CO} decreases slightly. In addition, the CH_4 conversion increases with increasing pressure.

It is important to note that this experiment was conducted at a constant mass flow rate, so the residence time of the gases in the monolith increased proportional to the absolute pressure. Thus, the observed increase in $S_{C_2H_4}$ and $S_{C_2H_6}$ could be partially due to increasing residence time. Longer residence times might allow more of the unreacted CH_4 to adsorb dissociatively and form $CH_x^{\cdot}$ radicals, which are believed to be the precursors to the products of oxidative coupling.

In addition, longer residence times would allow the water–gas shift reaction (3) to move the composition of the product gases closer to thermodynamic equilibrium. For these experiments, equilibrium requires a shift toward increasing concentrations of H_2 and CO_2, so the increase in S_{H_2} and the corresponding decrease in S_{CO} can be attributed to the water–gas shift reaction. Likewise, the slight increase in CH_4 conversion can be partially attributed to the slow progress of the steam reforming reaction (1) toward essentially complete equilibrium conversion of CH_4.

4. Discussion

4.1. Rh VERSUS Pt

As with Pt [2], the primary mechanism of formation of H_2 and CO on Rh must be methane pyrolysis. Thus, H_2 and CO can be formed in the following reaction sequence:

$$CH_{4,g} \rightarrow CH_{x,s} + (4-x)H_s, \tag{7a}$$

$$2H_s \rightarrow H_{2,g}, \tag{7b}$$

$$O_{2,g} \rightarrow 2O_s, \tag{7c}$$

$$C_s + O_s \rightarrow CO_s \rightarrow CO_g. \tag{7d}$$

However, any reactions involving OH, such as

$$CH_{x,s} + O_s \rightarrow CH_{x-1,s} + OH_s, \tag{8a}$$

$$H_s + O_s \rightarrow OH_s, \tag{8b}$$

$$OH_s + H_s \rightarrow H_2O_g \tag{8c}$$

$$CO_s + O_s \rightarrow CO_{2,g}, \tag{8d}$$

should all lead *almost inevitably* to H_2O and CO_2 because reverse reactions of these products are slow or thermodynamically unfavorable.

The superiority of Rh over Pt for synthesis gas formation must be because one or more of the surface reaction steps (8) involving OH is slower on Rh than on Pt. In fact, the difference in H_2 selectivity between Pt and Rh can be explained by the relative instability of the OH species on Rh surfaces. For the H_2–O_2–H_2O reaction system on both Pt and Rh, the elementary reaction steps have been identified and reaction rate parameters have been determined using laser induced fluorescence (LIF) to monitor the formation of OH radicals during hydrogen oxidation and water decomposition at high surface temperatures. These results have been fitted to a model based on the mechanism [7,8].

From these LIF experiments, it has been demonstrated that the formation of OH by reaction (8b) is much less favorable on Rh than on Pt (activation energies of 20 kcal/mol on Rh and 2.5 kcal/mol on Pt). This explains why Rh catalysts give significantly higher H_2 selectivities than Pt catalysts in our methane oxidation experiments.

Although the primary reason for the experimentally observed differences between Rh and Pt appears to be the very different activation energies for OH_s formation, other steps in the above mechanism may be quite different for the two metals. It is well known that methane adsorption on Pt and Rh is an activated process [9–12]. Since the rate of CH_4 adsorption, reaction (7a), is accelerated exponentially by higher temperatures, while the surface coverage of O_s adatoms decreases with higher temperatures, the ratio of $CH_{x,s}$ and H_s to O_s surface species will increase with higher temperatures. As the surface becomes more and more depleted of O_s adatoms, the rates of H_2O and CO_2 formation decrease relative to the rates of H_2 and CO formation.

If the rate of CH_4 chemisorption were different for the two metals, this would also influence the difference in observed selectivities. Experiments examining CH_4 adsorption on Rh films have shown that CH_4 chemisorption has an activation energy of ≈ 5 kcal/mol [9]. Although similar experiments for polycrystalline Pt or Pt(111) have not been reported, semiempirical electronic structure calculations for small clusters estimate an activation energy of dissociative chemisorption of 10.3 kcal/mol [13]. In addition, measurements of CH_4 dissociative adsorption give an apparent activation energy of 14.4 kcal/mol on Pt(110)-(1 × 2) [14] and 9.9 kcal/mol on Pt(100) [12]. Therefore, Rh also may be a better catalyst because of its ability to better facilitate breaking of the C–H bond during CH_4 chemisorption.

4.2. CATALYST MICROSTRUCTURE

With high metal loadings (≈ 10 wt%) on the monoliths, the catalytic activity appears to be primarily due to reactions on the metal surfaces, with relatively little influence from the support material. Since the initial fresh catalyst is

essentially covered with noble metal particles, relatively small changes in S_{H_2}, S_{CO}, and CH_4 conversion ($< 5\%$) with time suggest that most of the reaction is occurring on the noble metal surfaces even after significant changes in microstructure have occurred.

Nevertheless, these changes in microstructure result in exposure of the Al_2O_3 substrate to the reaction gases. In addition, higher loadings of metal correspond to less exposed substrate and better selectivities. These two observations indicate that the catalyst microstructure can have an important effect on CH_4 oxidation selectivity. Furthermore, these results suggest that the catalytic activity of exposed Al_2O_3 may be responsible for decreases in S_{H_2} which are observed with lower metal loadings or with microstructural changes that occur during reaction.

4.3. GAS PHASE REACTIONS

In addition to generation of undesired H_2O and CO_2 on the noble metal surfaces, the formation of these species and higher hydrocarbons in the gas phase may influence the observed selectivities and conversions. Experiments in empty quartz tubes at atmospheric pressure have demonstrated that methane may be converted to the carbon oxides and C_2 hydrocarbons at temperatures as low as 650°C [15]. Gas phase reactions will result in a mixture of several species, including the undesired combustion byproducts H_2O and CO_2, and are thus undesirable in a direct partial oxidation reactor.

For our atmospheric pressure experiments, the best indicators of the possible presence of gas phase reactions are C_2 hydrocarbons in the product gases. Typical selectivities for C_2H_4 and C_2H_6 are shown in fig. 4. Fig. 4a demonstrates that the production of C_2H_4 and C_2H_6 varies significantly with the catalyst chosen, but the overall selectivity of C_2 formation is always much less than 5%. In general, higher C_2 selectivities are observed for Pt catalysts than for Rh catalysts, and higher loadings of Rh reduce the generation of C_2 species. In fact, the 9.8 wt% Rh catalyst did not generate any detectable hydrocarbons.

The dependence of $S_{C_2H_4}$ and $S_{C_2H_6}$ on the catalyst used is probably a direct consequence of the autothermal reactor temperatures. Since Pt gives significantly lower S_{H_2} than Rh for a given feed composition and temperature, the adiabatic temperature increase due to reaction is significantly higher. This results in higher autothermal temperatures than with a Rh catalyst, such as shown in fig. 1d. Since the rates of gas phase reactions increase exponentially with temperature, they should be much faster for Pt catalysts than for Rh catalysts.

Extrapolation of these results to higher pressures is important since an industrial reactor would be expected to operate at pressures as high as 30 atm. The results in fig. 4 suggest that at reactor pressures of 1 to 2 atm, gas phase reactions only affect the reaction selectivity slightly. For all catalysts studied in

this research, none produced hydrocarbons at high enough levels to suggest that gas phase reactions play a major role in these experiments. Thus, a high pressure reactor for synthesis gas production from methane over Rh would be expected to give the high selectivities resulting from the methane pyrolysis surface reaction mechanism.

5. Summary

We have demonstrated that hydrogen and carbon monoxide can be produced in residence times of less than 10^{-2} s over Rh catalysts with H_2 and CO selectivities as high as 90 and 95%, respectively. The predominance of surface reactions over competing gas phase reactions is evidenced by the very low levels of hydrocarbons produced and by the high hydrogen selectivities, which are a function of both the catalytic species and the catalyst loading. The large improvement in S_{H_2} obtained by using Rh instead of Pt can be attributed to the much slower rate of OH formation on Rh surfaces. These very short residence times argue that H_2 is formed by a direct oxidation process rather than by $CH_4 + H_2O$ or $CH_4 + CO_2$ reactions because H_2O and CO_2 would have to form in a primary reaction. However, it is possible that some H_2 is formed by these reactions at high temperatures.

These results have significant applied and fundamental implications. The high selectivities and CH_4 conversions suggest that a new industrial process for synthesis gas production by direct oxidation of methane may be developed, and the differences between Pt and Rh suggest that these effects can be explained by known adsorption and reaction steps on these surfaces.

Acknowledgement

EAH was supported by an Upjohn Company Fellowship.

References

[1] M.V. Twigg, ed., *Catalyst Handbook* (Wolfe, London, 1989).
[2] D.A. Hickman and L.D. Schmidt, Synthesis gas formation by direct oxidation of methane over Pt monoliths, J. Catal. 138 (1992), in press.
[3] R.F. Blanks, T.S. Wittrig and D.A. Peterson, Chem. Eng. Sci. 45 (1990) 2407.
[4] D. Dissanayake, M.P. Rosynek, K.C.C. Kharas and J.H. Lunsford, J. Catal. 132 (1991) 117.
[5] A.T. Ashcroft, A.K. Cheetham, J.S. Foord, M.L.H. Green, C.P. Grey, A.J. Murrell and P.D.F. Vernon, Nature 344 (1990) 319.
[6] P.D.F. Vernon, M.L.H. Green, A.K. Cheetham and A.T. Ashcroft, Catal. Lett. 6 (1990) 181.
[7] W.R. Williams, C.M. Marks and L.D. Schmidt, Steps in the reaction $H_2 + O_2 \leftrightarrow H_2O$ on Pt: OH desorption at high temperatures, J. Phys. Chem. (1992), in press.

[8] M.P. Zum Mallen, W.R. Williams and L.D. Schmidt, Steps in H_2 oxidation on Rh: OH desorption at high temperatures, J. Phys. Chem., submitted.
[9] S.G. Brass and G. Ehrlich, Surf. Sci. 1987 (1987) 21.
[10] S.G. Brass and G. Ehrlich, Surf. Sci. 191 (1987) L819.
[11] S.G. Brass and G. Ehrlich, J. Chem. Phys. 87 (1987) 4285.
[12] A.C. Luntz and D.S. Bethune, J. Chem. Phys. 90 (1989) 1274.
[13] A.B. Anderson and J.J. Maloney, J. Phys. Chem. 92 (1988) 809.
[14] Y.-K. Sun and W.H. Weinberg, J. Vac. Sci. Technol. A8 (1990) 2445.
[15] G.S. Lane and E.E. Wolf, J. Catal. 113 (1988) 144.